Available online at www.sciencedirect.com
SCIENCE DIRECT®
Journal of Chromatography A, 1018 (2003) 233–249
JOURNAL OF CHROMATOGRAPHY A
www.elsevier.com/locate/chroma

Computer-assisted choice of discrete spacers for anionic isotachophoresis separations

Jozef Marák [a], Iveta Nagyová [b], Dušan Kaniansky [a,*]

[a] *Department of Analytical Chemistry, Faculty of Natural Sciences, Comenius University, Mlynská Dolina CH-2, SK-842 15 Bratislava, Slovak Republic*
[b] *Department of Chemistry, Faculty of Natural Sciences, Matej Bel University, Tajovského 40, SK-974 01 Banská Bystrica, Slovak Republic*

Received 20 May 2003; received in revised form 1 August 2003; accepted 7 August 2003

Abstract

In isotachophoresis (ITP), the sample constituents migrate, depending on their concentrations in the loaded sample, either in fully developed zones or in the boundary layers between the zones of constituents of the corresponding effective mobilities. The latter (spike) migration mode is analytically beneficial in selective detections of trace analytes, especially, when appropriately chosen discrete spacers minimize detection interferences due to matrix constituents. To facilitate a search for suitable mixtures of discrete spacers, a two-step calculation procedure was developed in this work. Using a pool of discrete spacers consisting of 42 anionic and zwitterionic constituents, this procedure was shown effective in the anionic ITP separations performed at pH = 6.5–10.0. Besides the predictions of the migration orders, it was helpful in identifying the spacing constituents that could cause resolution problems due to an uncertainty with which pH of the leading electrolyte solution is known. The ionic mobility and pK_a data, taken for the spacing constituents from the literature and the ones obtained from the ITP experiments carried out in this work, were used in the calculations performed in a context with the choice of spacers. Although the data obtained from the ITP experiments provided better results, small uncertainties with which they were acquired (attributable to fluctuations in the experimental conditions) set practical limits in the calculation based choice of multi-component mixtures of the spacing constituents.

Keywords: Isotachophoresis; Discrete spacers; Migration order prediction

1. Introduction

Separated constituents form in isotachophoresis (ITP), depending on their concentrations in the loaded sample, either fully developed zones or occupy, as spikes, the boundary layers between the zones of constituents of the corresponding effective mobilities [1–4]. The latter (spike) migration mode is typical for trace analytes in ITP and in combinations with UV-absorbance photometric (see, e.g. [3–21]), radiometric [22,23] and amperometric [24,25]) detectors provides favorable conditions for their sensitive detections. Here, the use of appropriately chosen spacing constituents enhances its practical utility as these reduce interferences in the detection of the analytes due to co-migrating matrix constituents.

* Corresponding author. Tel.: +421-2-60296-379; fax: +421-2-65425-360.
E-mail address: kaniansky@fns.uniba.sk (D. Kaniansky).

0021-9673/$ – see front matter © 2003 Elsevier B.V. All rights reserved.
doi:10.1016/j.chroma.2003.08.030

The use of discrete spacers is beneficial in preparative ITP [11,26–29] as well. Here, they define the analyte containing fraction in the ITP stack and, in addition, eliminate fluctuations in the matrix compositions of the trapped fraction(s) in repeated runs with the same sample [29]. In CZE with on-line ITP sample pretreatment, appropriately chosen discrete spacers restrict transfer of the matrix constituents to the CZE column and, consequently, contribute to favorable conditions in the final CZE separation and detection of trace analytes [30–33]. ITP in the column-coupling equipment can provide two-dimensional ITP separations when a suitable combination of discrete spacers is employed [34].

To simplify a search for suitable spacing constituents, multi-component mixtures of carrier ampholytes as developed for isoelectric focusing are recommended, especially, in the ITP separations of proteins (see, e.g. [4,7,9]). Unfortunately, this straightforward approach is less convenient as, for example, some of the macroconstituents of a particular ampholytic mixture can significantly dilute the separated constituents (carrier effects) while constituents of required effective mobilities need not be present in this mixture. Advantages of the use of discrete spacers in the ITP analysis of various groups of low molecular weight compounds [10,13–15,19], proteins [12,27,35–39] and complex ionic mixtures of natural origins [17,21] are known. Currently, this approach is less practical as the choice of discrete spacers of desired migration properties requires an experimentally demanding search, especially, for a multi-analyte problem. ITP steady-state models (see, e.g. [1,40–43]) and models describing dynamics of the ITP separation [44,45] offer predictive capabilities that can make the choice more effective. It is also important that experimental ITP procedures are available [1,2,40,41,46–52] that provide means to solutions of problems due to a lack of electromigration data for the constituents that can be used as discrete spacers.

The calculations of the steady-state parameters of the zones in the ITP separations based on differences in the (actual) ionic mobilities and pK values of the separated constituents [1,2], complemented by predictions of the migration orders of the zones in the ITP stacks [2,53], are relatively simple and rapid. Their results, however, need not agree with the corresponding ITP experiments. This can be, for example, due to the fact that the effective mobilities of the separated constituents are sensitive to ionic strength effects [54,55] that cannot be exactly included into the relationships between the effective and absolute ionic mobilities. In addition, risks of significant differences between the predicted (simulated) and actual ITP separations can be expected for multi-component mixtures when these contain the constituents of very close migration properties.

This work was aimed at developing a procedure suitable to the choice of discrete spacers by combining a two-step calculation procedure (the calculation of the steady-state parameters of the ITP zones of the constituents of interest [1] followed by a prediction of their migration order in the ITP stack with a simultaneous identification of the migration anomalies [34,53,56]) with a limited number of complementary ITP experiments. Here, the ITP experiments are intended to provide references with which the calculated data and predictions can be compared and, at the same time, as sources of primary data for the calculations of the (actual) ionic mobilities and pK_a values of the studied constituents to complement the data available in the literature (see, e.g. [42,49,50,52,57] and references given therein).

The spacers are often used in the anionic ITP separations performed at high pH values (e.g. in the separations of proteins) and, therefore, our attention was focused on the pH range of 6.5–10.0 while taking, mainly, amino acids, synthetic amino acids (Good buffers) and dipeptides as the spacing constituents. The anionic ITP separations carried out at such pH values may be adversely affected by high or variable contents of carbonate in the electrolyte solutions [58]. Although this is complicating comparisons of the experimental and calculated data, it is apparent that an evaluation of the proposed procedure under such critical conditions can demonstrate its real utility.

2. Theoretical background

2.1. Predictions of the migration order of discrete spacers in the ITP stack

A drawing in Fig. 1 illustrates the spike mode of ITP migration of the analyte (A) in the boundary layer between the zones of the spacing constituents (SX

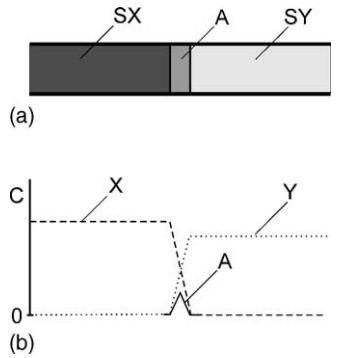

Fig. 1. A schematic view of the ITP migration of the analyte (A) in the boundary layer between the zones of front (X) and rear (Y) spacing constituents: (a) an illustration of the situation in the capillary tube; and (b) concentration distributions of the analyte and spacing constituents along the capillary tube.

and SY). This migration configuration, typical for the spacing constituents, requires that the following conditions are met [2,34,53]:

$$\bar{m}_{X,SY} > \bar{m}_{Y,SY} \quad (1a)$$

$$\bar{m}_{Y,SX} < \bar{m}_{X,SX} \quad (1b)$$

and

$$\bar{m}_{A,SY} > \bar{m}_{Y,SY} \quad (2a)$$

$$\bar{m}_{A,SX} < \bar{m}_{X,SX} \quad (2b)$$

where $\bar{m}$ is a symbol for the effective mobility and the first subscripts relate to the constituents while the second subscripts identify their zones.

The conditions (1a) and (1b) determine, for particular separating conditions, the migration order of a pair of the constituents forming fully developed zones in the ITP stack [2,34,53]. On the other hand, the conditions (2a) and (2b) are relevant to the migration of the analyte focused in the boundary layer between such a pair of the zones [34]. A corresponding set of the conditions is needed in examinations of the migration order of multi-component mixtures of the separated constituents [53,56].

Current versions of the ITP steady-state model (see, e.g. [1,40,42] and references given therein) are usually employed to calculations of the steady-state data of the zones of the separated constituents. As such, they neither provide their migration orders in the ITP stack nor identify explicitly migration anomalies that may occur in their ITP separations [53,59]. Implementations of the conditions (1a) and (1b) along with definition conditions of the migration anomalies in the ITP stack [53] into the steady-state model is straightforward [56] and this step extends its use also to computation based predictions of the migration orders and assessments of the ITP separabilities of (multi-component) mixtures.

2.2. Acquisitions of the effective mobilities of the constituents from their ITP separations

The calculations of the effective mobilities and predictions of the migration orders of the separated constituents in ITP require that the actual (or absolute) ionic mobilities of the ionic forms of the separated constituents and the corresponding dissociation constants are available [1,2,40,42]. Although for some constituents that can serve as discrete spacers in ITP these constants can be found in the literature (see, e.g. [42,50,52] and references given therein), there is a general lack of these fundamental data. In addition, the literature values for some constituents may scatter significantly (see below) and a correct choice may be difficult. These limitations can be overcome by using one of the procedures as elaborated for their experimental acquisitions by ITP [1,2,40,41,46–52]. To perform the acquisition effectively, the data should be obtained from the ITP separations of multi-component mixtures of the constituents of interest. This approach, providing besides the effective mobilities of the constituents also their actual migration orders in the ITP stacks, makes possible comparisons of relevant experimental and calculated data. From an overview of the ITP methods proposed to the measurements of mobilities and dissociation constants [52], it is apparent that such requirements are met best by the ones making the use of the response of the ITP universal detectors.

For reasons mentioned in the previous paragraph, the use of conductivity detection to the acquisitions of the ionic mobilities and pK_a values from the ITP separations of the studied constituents (discrete spacers) was preferred in this work. Here, some specificities of the conductivity detection have to be taken into account [1,2,60]. For example, the signal amplitudes (plateaus) as obtained for the separated constituent by the contact conductivity detector (see Fig. 2) in repeated ITP runs slightly deviate also in instances when

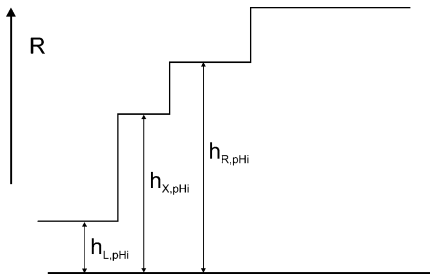

Fig. 2. Definitions of the heights of the plateaus of the leading ($h_{\mathrm{L,pH}_i}$), spacing ($h_{\mathrm{X,pH}_i}$) and reference ($h_{\mathrm{R,pH}_i}$) zones on an isotachopherogram as used in the calculations of the RSH values from the response of the conductivity detector.

the detector operates correctly. These deviations can be ascribed to small changes in the states of surfaces of the detection electrodes due to adsorption and electrochemical processes [1,60]. In addition, run-to-run temperature fluctuations can play a certain role as well. To minimize impacts of these disturbances on the detection data, it is convenient to employ a relative scale (relative stepheights, RSH values), defined for a particular constituent (X) in the following way [1,61]:

$$\mathrm{RSH}_{\mathrm{X(R),pH}_i} = \frac{h_{\mathrm{X,pH}_i} - h_{\mathrm{L,pH}_i}}{h_{\mathrm{R,pH}_i} - h_{\mathrm{L,pH}_i}} \tag{3}$$

where $h_{\mathrm{X,pH}_i}$, $h_{\mathrm{R,pH}_i}$ and $h_{\mathrm{L,pH}_i}$ are the amplitudes of the detection signal (Fig. 2) of the spacing (X), reference (R) and leading (L) constituents at a given pH value (pH_i), respectively. The signal amplitude for the spacing constituent is in a relationship with the specific electric conductivity of its zone ($\kappa_{\mathrm{X,pH}_i}$) when the detector operates in the resistance measurement mode:

$$h_{\mathrm{X,pH}_i} = kC \cdot \frac{1}{\kappa_{\mathrm{X,pH}_i}} \tag{4}$$

where C is a symbol for the resistance cell constant and k a proportionality constant.

Ohm's law and the ITP condition of migration give [1,2]:

$$\kappa_{\mathrm{X,pH}_i} = \frac{J}{v_{\mathrm{pH}_i}} \cdot \bar{m}_{\mathrm{X,pH}_i} \tag{5}$$

where J is the current density, $\bar{m}_{\mathrm{X,pH}_i}$ the effective mobility of the constituent of interest under particular separating conditions and v_{pH_i} is a symbol for the steady-state velocity of the zones present in the ITP stack.

Substitutions from Eqs. (4) and (5) convert Eq. (3) into the following form [61]:

$$\mathrm{RSH}_{\mathrm{X(R),pH}_i} = \frac{\bar{m}_{\mathrm{R,pH}_i}}{\bar{m}_{\mathrm{L,pH}_i} - \bar{m}_{\mathrm{R,pH}_i}} \left(\frac{\bar{m}_{\mathrm{L,pH}_i}}{\bar{m}_{\mathrm{X,pH}_i}} - 1 \right). \tag{6}$$

Rearranged Eq. (6)

$$\bar{m}_{\mathrm{X,pH}_i} = \frac{\bar{m}_{\mathrm{L,pH}_i} \cdot \bar{m}_{\mathrm{R,pH}_i}}{\mathrm{RSH}_{\mathrm{X(R),pH}_i}(\bar{m}_{\mathrm{L,pH}_i} - \bar{m}_{\mathrm{R,pH}_i}) + \bar{m}_{\mathrm{R,pH}_i}} \tag{7}$$

allows the calculation of the effective mobility of the constituent X, for a particular leading electrolyte (identified via pH_i), from its $\mathrm{RSH}_{\mathrm{X(R),pH}_i}$ value when the effective mobilities of the leading ($\bar{m}_{\mathrm{L,pH}_i}$) and reference ($\bar{m}_{\mathrm{R,pH}_i}$) constituents are available or computable.

2.3. Calculations of the ionic mobilities and pK_a values from the effective mobilities of the constituents

A definition equation of the effective mobility of the constituent forming n ionic forms, when only its acid–base properties are important from the point of view of the electrophoretic migration, gives [1,2,40]:

$$\bar{m}_{\mathrm{H}_n\mathrm{X,pH}_i} = \sum_{f=1}^{n} \frac{\prod_{f=1}^{f} K_{\mathrm{H}_n\mathrm{X},f} / [\mathrm{H}^+]_{\mathrm{X,pH}_i}^{f}}{1 + \sum_{f=1}^{n} \left(\prod_{f=1}^{f} K_{\mathrm{H}_n\mathrm{X},f} / [\mathrm{H}^+]_{\mathrm{X,pH}_i}^{f} \right)} \times m_{\mathrm{H}_{n-f}\mathrm{X}} \tag{8}$$

Eq. (8) can be used in the calculations of the ionic mobilities of the ionic forms of the constituent ($m_{\mathrm{H}_{n-1}\mathrm{X}}$, $m_{\mathrm{H}_{n-2}\mathrm{X}}, \ldots, m_{\mathrm{H}_{n-f}\mathrm{X}}, \ldots, m_{\mathrm{X}}$) and the corresponding dissociation constants ($K_{\mathrm{H}_n\mathrm{X},1}$, $K_{\mathrm{H}_n\mathrm{X},2}, \ldots, K_{\mathrm{H}_n\mathrm{X},f}, \ldots, K_{\mathrm{H}_n\mathrm{X},n}$) from the effective mobilities obtained experimentally with the leading electrolytes of different pH values. Here, the second subscript in the term $[\mathrm{H}^+]_{\mathrm{X,pH}_i}^{f}$, expressing the concentration of H^+ ion in the zone of X when a particular leading electrolyte is employed (identified via pH_i), stresses the fact that the pH values in the ITP zones differ from that of the leading electrolyte [1,2].

From Eq. (8), it is apparent that the effective mobility of a strong ionic constituent is identical with the actual ionic mobility of its dominant ionic form at all relevant pH values. For the effective mobility of a monovalent, weakly ionic constituent, HX, Eq. (8) reduces to:

$$\bar{m}_{\mathrm{HX,pH}_i} = \frac{K_{\mathrm{HX}}}{K_{\mathrm{HX}} + [\mathrm{H}^+]_{\mathrm{X,pH}_i}} \cdot m_{\mathrm{X}} \quad (9)$$

Eq. (9) rearranged into a form

$$\frac{1}{\bar{m}_{\mathrm{HX,pH}_i}} = \frac{1}{m_{\mathrm{X}}} + \frac{1}{K_{\mathrm{HX}} \cdot m_{\mathrm{X}}} \cdot [\mathrm{H}^+]_{\mathrm{X,pH}_i} \quad (10)$$

provides means for the calculation of m_{X} and K_{HX} from a plot of $1/\bar{m}_{\mathrm{HX,pH}_i}$ versus $[\mathrm{H}^+]_{\mathrm{X,pH}_i}$.

For the effective mobility of a divalent, weakly ionic constituent Eq. (8) reduces to:

$$\bar{m}_{\mathrm{H_2X,pH}_i} = \frac{\begin{array}{c} K_{\mathrm{H_2X},1} \cdot [\mathrm{H}^+]_{\mathrm{X,pH}_i} \cdot m_{\mathrm{HX}} \\ + K_{\mathrm{H_2X},1} \cdot K_{\mathrm{H_2X},2} \cdot m_{\mathrm{X}} \end{array}}{\begin{array}{c} [H^+]^2_{\mathrm{X,pH}_i} + K_{\mathrm{H_2X},1} \cdot [\mathrm{H}^+]_{\mathrm{X,pH}_i} \\ + K_{\mathrm{H_2X},1} \cdot K_{\mathrm{H_2X},2} \end{array}}. \quad (11)$$

Here, a plot of $\bar{m}_{\mathrm{H_2X,pH}_i}$ versus $[\mathrm{H}^+]_{\mathrm{X,pH}_i}$ and a suitable numerical fitting procedure provide the ionic mobilities of the single (m_{HX}) and double (m_{X}) charged ionic forms and the corresponding dissociation constants ($K_{\mathrm{H_2X},1}$ and $K_{\mathrm{H_2X},2}$) from the effective mobilities obtained for H_2X at different pH values of the leading electrolyte. It is apparent that the use of Eq. (8) can be extended to the calculations of the ionic mobilities and pK_a values of higher multivalent weakly ionic constituents as well.

3. Materials and methods

3.1. Instrumentation

An ITAChrom EA 101 capillary electrophoresis analyzer (J&M, Aalen, Germany) was used in our experiments. It was assembled with the column-coupling configuration of the separation unit using modules supplied by the manufacturer. The preseparation column was provided with a 800 μm i.d. capillary tube made of fluorinated ethylene–propylene copolymer (FEP). The length of the capillary tube was 90 mm.

A 300 μm i.d. capillary tube made of FEP (160 mm in the length) was used in the analytical column. The columns were kept at ambient temperature (21–23 °C, in experiments performed in this work). The driving currents were stabilized at 200 and 40 μA in the preseparation and analytical columns, respectively. The sample solutions were injected into the analyzer with the aid of a 30 μl loop of the injection valve.

3.2. Chemicals and electrolyte solutions

The leading and terminating electrolyte solutions (Table 1) were prepared from chemicals obtained from Serva (Heidelberg, Germany), Sigma Chemical Co. (St. Louis, MO, USA) and Merck (Darmstadt, Germany). Hydroxyethylcellulose (HEC; Serva) served as an electro-osmotic flow (EOF) suppressor. Aqueous stock solutions of the discrete spacers (Table 2) were prepared from chemicals provided by the above suppliers.

Absorption of CO_2 by the electrolyte solutions was prevented by keeping the solutions in closed vessels and permanently placed in a desiccator over NaOH pellets. The terminating electrolyte solution in the terminating electrode compartment of the analyzer was maintained in a closed environment using a gas proof cap. The ambient pressure above the solution in the compartment was preserved via a microcolumn packed with NaOH pellets. The microcolumn was tightly connected to the electrode compartment via a Luer female connector in the cap.

3.3. Prediction of the RSH values of the spacing constituents and their migration order in the ITP stack

The migration orders of the spacing constituents in the ITP stacks were predicted with the aid of the program ORDER [56]. In addition, this program made possible identifications of the migration anomalies that can occur in the ITP stack [53] and, including the program ITER [1], it provided, for a given electrolyte system and relevant input data, the steady-state parameters of the ITP zones of the spacing constituents and their RSH values.

Table 1
Electrolyte systems

	Electrolyte system number							
	1	2	3	4	5	6	7	8
Leading electrolyte								
Solvent	H_2O	H_2O	H_2O	H_2O	H_2O	H_2O	H_2O	H_2O
Anion	Cl^-	Cl^-	Cl^-	Cl^-	Cl^-	Cl^-	Cl^-	Cl^-
Mobility ($\times 10^5$ cm^2 V^{-1} s^{-1})	79.1							
Concentration (mmol/l)	10	10	10	10	10	10	10	10
Counter ion	Histidine	Imidazole	Imidazole	Tris	Tris	BTP	BTP	Ethanolamine
Mobility ($\times 10^5$ cm^2 V^{-1} s^{-1})	29.6	52.0	52.0	29.5	29.5	21.6	21.6	44.3
pK_a	6.04	7.15	7.15	8.08	8.08	9.00	9.00	9.50
EOF suppressor	HEC	HEC	HEC	HEC	HEC	HEC	HEC	HEC
Concentration (%, w/v)	0.2	0.2	0.2	0.2	0.2	0.2	0.2	0.2
pH	6.50	7.00	7.50	8.00	8.50	9.00	9.50	10.00
Terminating electrolyte								
Solvent	H_2O	H_2O	H_2O	H_2O	H_2O	H_2O	H_2O	H_2O
Anion	MOPS	Bicine	Bicine	Threonine	Glycine	Glycine	OH^- (H_2O)	OH^- (H_2O)
Concentration (mmol/l)	5	5	5	5	5	5	–	–
Counter ion	Histidine	Imidazole	Imidazole	Tris	Tris	BTP	–	–
Concentration (mmol/l)	2.5	2.5	2.5	2.5	2.5	2.5	–	–

The ionic mobility and pK_a data were taken from the literature [42,49,50,52,57,67]; HEC: hydroxyethylcellulose; BTP: 1,3bis[tris (hydroxymethyl)-methylamino]propane.

3.4. Calculations of the effective and ionic mobilities and pK_a values of the spacing constituents from experimental ITP data

An iterative calculation procedure (see a flow-chart in Fig. 3) provided the effective mobilities and, subsequently, ionic mobilities and pK_a values of the spacing constituents from the experimental ITP data as obtained in this work. Here, the calculations were performed in Excel (Microsoft, Redmond, WA, USA), WinCurveFit (v.1.0b1, Kevin Raner, MtWaverly, Australia) and ORDER [56].

4. Results and discussion

When the resolving power characteristic for ITP [62] is considered, it is reasonable to assume that a certain number of appropriately chosen ionogenic constituents may serve as a pool for mixtures of discrete spacers of required electromigration properties for a broader pH range. With this fact in mind, a group of 42 anionic and zwitterionic constituents was chosen into our study (Table 2). This choice took into account, besides acid–base properties and (absolute) ionic mobilities (see Table 3), also minimum UV light absorptivities of these constituents. Therefore, while providing spacing effects within a broad range of the effective mobilities in the anionic ITP separations at pH = 6.5–10.0, they are, at the same time, compatible, at least, with photometric absorbance and fluorescence detections of trace analytes migrating in the ITP spike mode (Fig. 1). These properties also make them suitable for the selection of the analyte(s) containing fraction(s) from the ITP stack in instances when ITP is used as a sample pretreatment technique (e.g. in the ITP–CZE separations performed in the column-coupling separation system [30–33,63] and in HPLC with off-line ITP sample pretreatment [11,29]).

The electrolyte systems employed in this work (Table 1) covered, with 0.5 pH unit increments, the pH range of our interest (pH = 6.5–10.0). Their compositions reflected the fact that only the ITP separations according to differences in pK values and ionic mobilities [1] were studied. The choice of the leading and terminating anions favored the

Table 2
List of constituents providing a pool of discrete spacers for anionic ITP separations at pH = 6.5–10.0

Number	Spacing constituent	Code	Number	Spacing constituent	Code
1	Aminomethylsulfonic	AMSA	22	*N*-(2-Hydroxyethyl)-piperazine-*N*′-3-propanesulfonic	HEPPS
2	*N*-(2-Acetamido)-iminodiacetic	ADA	23	*N*,*N*-Bis(2-hydroxyethyl)-glycine	Bicine
3	Carbonic	Carb	24	Glycylleucine	Gly-Leu
4	Piperazine-*N*,*N*′-bis(2-ethanesulfonic)	PIPES	25	*N*-Tris(hydroxymethyl)methyl-3-aminopropanesulfonic	TAPS
5	Aspartic	Asp	26	Methioninesulphoxide	Metso
6	Glutamic	Glu	27	Asparagine	Asn
7	2-Aminoadipic	Amadp	28	Taurine	Tau
8	2-Aminopimelic	Apm	29	Threonine	Thr
9	Cacodylic	Cacd	30	Serine	Ser
10	2-(*N*-Morpholino)-ethanesufonic	MES	31	Boric	Boric
11	*N*-(2-Acetamido)-2-aminoethanesulfonic	ACES	32	2,6-Diaminopimelic	Dapm
12	3-(*N*-Morpholino)-2-hydroxypropanesulfonic	MOPSO	33	*N*-(1,1-Dimethyl-2-hydroxyethyl)-3-amino-2-hydroxy propanesulfonic	AMPSO
13	3-(*N*-Morpholino)-propanesulfonic	MOPS	34	Glycine	Gly
14	Piperazine-*N*,*N*′-bis(2-hydroxypropanesulfonic)	POPSO	35	2-(Cyclohexylamino)ethanesulfonic	CHES
15	*N*,*N*-Bis(2-hydroxyethyl)-2-aminoethanesulfonic	BES	36	Citruline	Cit
16	3-[*N*-Bis(2-hydroxyethyl)amino]-2-hydroxypropanesulfonic	DIPSO	37	Norvaline	Nval
17	N-(2-Hydroxyethyl)-piperazine-*N*′-2-ethanesulfonic	HEPES	38	Isoleucine	Ileu
18	3-[*N*-Tris(hydroxymethyl)methylamino]-2-hydroxy propanesulfonic	TAPSO	39	Norleucine	Nleu
19	Glycylglycine	Gly-Gly	40	β-Alanine	BALA
20	*N*-[Tris(hydroxymethyl)-methyl]-glycine	Tricine	41	Proline	Pro
21	*N*-(2-Hydroxyethyl)-piperazine-*N*′-2-hydroxy propanesulfonic	HEPPSO	42	3-(Cyclohexylamino)propanesulfonic	CAPS

constituents providing broad ranges of the effective mobilities within the ITP stacks. On the other hand, identical concentrations of the leading anions and the use of pH buffering counter-ionic constituents of an identical charge type [54] in the leading electrolyte solutions were employed to keep influences of the ionic strength on the ionic mobilities constant and, consequently, changes of the ionic mobilities within the studied pH interval negligible.

4.1. Choice of discrete spacers and pK_a and ionic mobility data

To select a group of spacers suitable for a particular analytical problem in a short time, we exploited fully predictions of the separabilities and migration orders of the studied constituents as provided by the computing procedure developed in a context of this work. This approach, however, cannot eliminate a need for a certain number of experiments, as the model employed and quality of the input data determine reliabilities of the predictions. To assess impacts of the input data on the predictions, we carried out ITP separations of mixtures of the studied constituents in the all electrolyte systems. The data obtained in this way (the RSH values, Table 4, and migration orders of the constituents in the ITP stacks) served as references with which the calculated RSH values and the predicted migration orders were compared. Deviations of the calculated RSH values from those obtained experimentally and, especially, disagreements in the predicted and actual migration orders of the constituents in the ITP stack indicated the use of incorrect input data in the calculations. The disagreements occurred, mainly, for mixtures of spacers in which the constituents of close migration properties were present. This, for example,

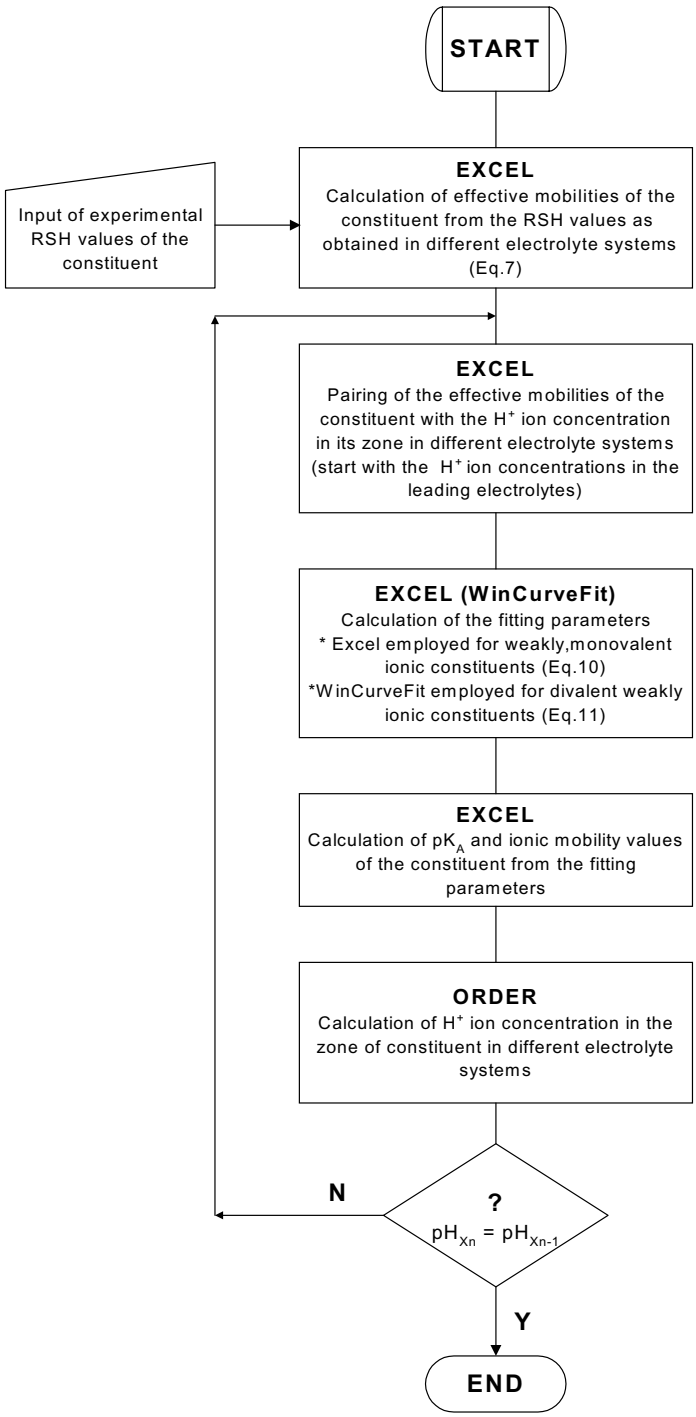

Fig. 3. A flow-chart of an iterative calculation of the ionic mobilities and pK_a values of the constituent from its experimental ITP data as provided by the conductivity detector of the analytical column under the electrolyte conditions described in Table 1.

Table 3
pK_a and ionic mobility data of the spacing constituents

Number	Spacer (*i*)	pK_a (range)[a]	pK_a (range)[b]	*m* (range)[a]	*m* (range)[b]
1	AMSA	5.75	6.07 (6.02–6.13)	–	44.0 (43.4–44.9)
2	ADA (2)	6.61 (6.60–6.62)	–	–	–
3	Carb (1)	6.35	–	46.1	–
	Carb (2)	10.33	–	71.8	–
4	PIPES (1)	2.81	2.81	–	
	PIPES (2)	6.73 (6.66–6.80)	6.37 (6.33–6.37)	–	41.6 (40.7–42.1)
5	Asp (1)	3.90	3.90	30.9 (30.1–31.6)	30.9
	Asp (2)	9.97 (9.90–10.02)	10.00	54.7 (51.8–56.8)	55.4
6	Glu (1)	4.30 (4.07–4.42)	4.32	27.4 (25.4–28.9)	28.5
	Glu (2)	9.80 (9.47–9.97)	9.96	53.2 (49.6–55.7)	53.0
7	Amadp(1)	4.21	4.21	–	26.8
	Amadp (2)	9.77	9.77	–	44.0
8	Apm (1)	–	4.30	–	25.0
	Apm (2)	–	9.80	–	44.0
9	Cacd	6.21 (6.18–6.27)	6.33 (6.28–6.33)	29.9	30.3 (29.4–30.9)
10	MES	6.14 (6.10–6.20)	6.18 (6.12–6.23)	27.4 (26.8–28.0)	28.3 (27.4–29.1)
11	ACES	6.86 (6.84–6.90)	6.84 (6.78–6.86)	31.3	30.6 (29.9–31.0)
12	MOPSO	6.85 (6.75–6.95)	6.95 (6.95–6.96)	23.8	26.6 (26.0–27.3)
13	MOPS	7.18 (7.16–7.20)	7.23 (7.22–7.23)	24.4	26.9 (26.3–27.6)
14	POPSO (2)	7.76 (7.63–7.85)	7.26 (7.24–7.26)	–	36.9 (35.9–37.9)
15	BES	7.15 (7.10–7.17)	7.22 (7.21–7.23)	24.0	26.7 (26.2–27.3)
16	DIPSO	7.48 (7.35–7.60)	7.59 (7.57–7.59)	–	25.0 (24.2 –25.5)
17	HEPES	7.43 (7.31–7.55)	7.61 (7.59–7.63)	21.8	23.2 (22.7–23.8)
18	TAPSO	7.56 (7.39–7.70)	7.67 (7.66–7.67)	–	24.0 (23.1–24.8)
19	Gly-Gly	8.28 (8.20–8.40)	8.24 (8.21–8.29)	31.5	31.9 (31.2–32.2)
20	Tricine	8.13 (8.10–8.15)	8.15 (8.13–8.16)	–	26.6 (25.8–27.5)
21	HEPPSO	7.82 (7.51–8.00)	8.01 (7.96–8.02)	22.0	22.0 (21.5–22.5)
22	HEPPS	8.05 (8.00–8.10)	8.01 (7.95–8.01)	–	21.8 (21.2–22.2)
23	Bicine	8.33 (8.30–8.35)	8.25 (8.25–8.26)	–	26.5 (25.8–27.4)
24	Gly-Leu	8.43	8.16 (8.08–8.18)	25.1	23.9 (23.1–24.5)
25	TAPS	8.42 (8.30–8.55)	8.33 (8.32–8.33)	25.0	22.9 (22.0–23.6)
26	Metso	–	8.58 (8.57–8.60)	–	26.9 (26.2–27.6)
27	Aspn	8.94 (8.84–9.03)	8.79 (8.77–8.80)	31.6	30.1 (29.2–30.6)
28	Tau	9.18	8.89 (8.89–8.93)	37.9	35.0 (34.2–37.1)
29	Thr	9.18 (9.10–9.23)	9.05 (8.97–9.06)	31.3 (30.9–31.6)	30.0 (29.0 – 30.2)
30	Ser	9.24 (9.21–9.30)	9.10 (9.03–9.11)	33.6	31.5 (30.3–31.8)
31	Boric (1)	9.22 (9.20–9.24)	–	–	–
	Boric (2)	12.74	–	–	–
	Boric (3)	13.80	–	–	–
32	Dapim(1)	8.80	8.80	–	17.0
	Dapim (2)	9.90	9.90	–	37.0
33	AMPSO	9.05 (9.00–9.10)	8.95 (8.92–8.96)	–	22.1 (21.6–23.0)
34	Gly	9.78	9.92 (9.85–9.92)	37.4	41.4 (36.9–41.7)
35	CHES	9.45 (9.30–9.55)	9.48 (9.45–9.50)	–	25.1 (24.1–25.6)
36	Cit	–	9.53 (9.52–9.53)	–	24.2 (22.8–25.4)
37	Nval	–	9.69 (9.48–9.79)	–	25.4 (21.7–28.1)
38	Ileu	9.77	9.77 (9.60–9.88)	26.7	26.4 (25.5–26.5)
39	Nleu	–	9.71 (9.70–9.71)	–	23.8 (21.8–25.6)
40	BALA	10.26 (10.24–10.30)	10.24	30.8	29.2
41	Pro	10.64	10.64	25.4	27.0
42	CAPS	10.35 (10.30–10.40)	10.40	–	22.0

The numbers and codes identifying the spacers are identical with those used in Table 1. *i*: *i*th ionic form of the constituent; *m*: ionic mobility ($\times 10^5$ cm^2 V^{-1} s^{-1}).

[a] The data taken from [42,49,50,52,57].

[b] The data obtained from the ITP experiments performed in this work.

Table 4
RSH values of the spacing constituents obtained from the conductivity detection in the ITP runs performed at pH = 6.5–10.0

No.	Spacer	RSH value (range)							
		pH = 6.5	pH = 7.0	pH = 7.5	pH = 8.0	pH = 8.5	pH = 9.0	pH = 9.5	pH = 10.0
1	AMSA	0.88	1.00	1.00	1.11 (1.07–1.13)	1.15 (1.14–1.17)	1.23 (1.18–1.25)	1.42 (1.29–1.51)	1.80 (1.65–1.92)
2	ADA	0.91	1.00	1.00	1.00	1.00	1.00	1.09 (1.07–1.13)	1.29 (1.21–1.39)
3	Carb	1.00	1.00	1.00	1.00	1.00	1.00	1.00	1.00
4	PIPES	1.16 (1.11–1.19)	1.32 (1.27–1.35)	1.26 (1.23–1.30)	1.25 (1.23–1.29)	1.29 (1.24–1.36)	1.35 (1.33–1.37)	1.59 (1.55–1.66)	1.93 (1.85–2.12)
5	Asp	1.11 (1.10–1.13)	1.57 (1.53–1.64)	1.78 (1.73–1.84)	1.95 (1.90–2.01)	1.90 (1.85–1.95)	1.94 (1.91–1.96)	1.86 (1.77–1.93)	1.73 (1.60–1.92)
6	Glu	1.29 (1.27–1.31)	1.79 (1.74–1.84)	2.08 (1.94–2.14)	2.22 (2.19–2.27)	2.26 (2.14–2.45)	2.18 (2.15–2.21)	2.09 (1.95–2.25)	1.90 (1.74–2.07)
7	Amadp	1.48 (1.46–1.51)	2.04 (2.01–2.05)	2.35 (2.26–2.47)	2.56 (2.50–2.62)	2.68 (2.56–2.80)	2.60 (2.53–2.66)	2.50 (2.32–2.78)	2.35 (2.17–2.58)
8	Apm	1.61 (1.55–1.67)	2.29 (2.15–2.36)	2.58 (2.43–2.70)	2.81 (2.75–2.86)	2.93 (2.75–3.10)	2.88 (2.74–3.01)	2.78 (2.63–3.05)	2.70 (2.50–2.95)
9	Cacd	1.79 (1.69–1.85)	2.00 (1.89–2.11)	2.01 (1.94–2.06)	2.19 (2.13–2.20)	2.32 (2.24–2.45)	2.45 (2.38–2.51)	2.93 (2.81–3.15)	3.81 (3.60–4.05)
10	MES	1.80 (1.79–1.83)	2.07 (2.00–2.15)	2.30 (2.19–2.38)	2.40 (2.34–2.45)	2.54 (2.44–2.63)	2.70 (2.63–2.81)	3.19 (2.91–3.54)	4.34 (4.21–4.57)
11	ACES	2.60 (2.42–2.70)	2.44 (2.32–2.53)	2.30 (2.25–2.38)	2.23 (2.19–2.28)	2.27 (2.23–2.33)	2.41 (2.36–2.46)	2.88 (2.76–3.16)	3.73 (3.60–3.83)
12	MOPSO	3.31 (3.22–3.42)	3.12 (3.01–3.20)	2.90 (2.84–2.99)	2.80 (2.76–2.84)	2.86 (2.75–2.96)	3.03 (2.94–3.12)	3.34 (3.21–3.44)	4.74 (4.43–5.14)
13	MOPS		3.66 (3.53–3.76)	3.19 (3.07–3.29)	2.88 (2.83–2.93)	2.88 (2.75–3.02)	3.00 (2.96–3.04)	3.37 (3.23–3.48)	4.70 (4.43–4.94)
14	POPSO		2.43 (2.32–2.49)	2.36 (2.32–2.43)	2.02 (1.96–2.06)	1.74 (1.66–1.88)	1.71 (1.68–1.73)	1.94 (1.77–2.06)	2.43 (2.28–2.65)
15	BES		3.66 (3.56–3.78)	3.17 (3.07–3.31)	2.92 (2.86–2.97)	2.90 (2.75–3.07)	3.00 (2.90–3.09)	3.44 (3.40–3.52)	4.73 (4.59–4.88)
16	DIPSO		5.16 (4.97–5.34)	4.34 (4.18–4.46)	3.54 (3.46–3.61)	3.33 (3.25–3.57)	3.36 (3.26–3.47)	3.83 (3.80–3.85)	5.38 (5.04–5.89)
17	HEPES		5.72 (5.40–5.92)	4.73 (4.56–4.89)	3.87 (3.80–3.99)	3.76 (3.65–3.85)	3.76 (3.63–3.93)	4.30 (3.99–4.48)	5.94 (5.73–6.04)
18	TAPSO		5.79 (5.51–5.96)	4.74 (4.67–4.85)	3.81 (3.72–3.93)	3.63 (3.48–3.79)	3.60 (3.44–3.70)	4.12 (3.79–4.48)	5.66 (5.32–6.02)
19	Gly-Gly		7.42 (7.02–7.89)	5.83 (5.65–6.03)	3.76 (3.69–3.90)	3.10 (2.96–3.24)	2.70 (2.63–2.75)	2.92 (2.81–3.05)	3.63 (3.44–3.96)
20	Tricine		7.97 (7.63–8.43)	6.25 (6.06–6.41)	4.33 (4.22–4.46)	3.65 (3.56–3.74)	3.37 (3.25–3.48)	3.67 (3.40–4.05)	4.88 (4.60–5.41)
21	HEPPSO		8.24 (7.80–8.64)	6.62 (6.46–6.85)	5.01 (4.80–5.20)	4.39 (4.14–4.66)	4.30 (4.19–4.37)	4.58 (4.37–4.72)	6.39 (6.22–6.68)
22	HEPPS		8.26 (7.85–8.51)	6.55 (6.41–6.79)	4.99 (4.80–5.24)	4.37 (4.14–4.61)	4.35 (4.33–4.37)	4.77 (4.44–5.04)	6.53 (6.43–6.62)
23	Bicine				4.91 (4.82–5.06)	4.04 (3.85–4.40)	3.47 (3.38–3.53)	3.57 (3.36–3.68)	4.61 (4.43–4.81)
24	Gly-Leu				5.27 (4.82–5.54)	4.32 (4.14–4.53)	3.92 (3.75–4.05)	4.07 (3.80–4.24)	5.52 (5.32–5.88)
25	TAPS				6.21 (5.96–6.51)	4.91 (4.75–5.18)	4.33 (4.29–4.37)	4.34 (3.99–4.65)	5.96 (5.75–6.38)
26	Metso				6.33 (6.08–6.71)	4.75 (4.53–4.84)	3.78 (3.72–3.92)	3.74 (3.67–3.87)	4.66 (4.28–5.05)
27	Asn				6.71 (6.42–6.97)	5.00 (4.89–5.14)	3.78 (3.66–3.93)	3.28 (3.13–3.43)	3.87 (3.76–4.10)
28	Tau				6.44 (6.23–6.66)	4.59 (4.04–4.86)	3.24 (3.13–3.59)	2.80 (2.75–2.87)	3.10 (2.71–3.07)
29	Thr					6.15 (5.59–6.51)	4.33 (4.24–4.37)	3.80 (3.57–4.09)	4.06 (3.83–4.33)
30	Ser					6.11 (5.59–6.45)	4.32 (4.24–4.37)	3.62 (3.35–4.00)	3.69 (3.53–3.96)
31	Boric					7.07 (6.49–7.41)	–	10.74 (10.08–11.70)	3.34 (3.16–3.56)
32	Dapm					7.45 (7.04–7.72)	5.18 (5.09–5.29)	4.38 (4.14–4.78)	3.59 (3.33–3.96)
33	AMPSO					7.72 (7.19–8.03)	5.84 (5.75–5.96)	5.32 (4.92–5.49)	6.30 (5.80–6.58)
34	Gly							4.68 (4.38–5.02)	3.90 (3.72–4.34)
35	CHES							5.90 (5.65–6.29)	6.02 (5.82–6.39)
36	Cit							6.30 (6.00–6.73)	6.38 (6.03–6.85)
37	Nval							6.70 (6.49–6.92)	6.40 (5.94–7.18)
38	Ileu							6.83 (6.27–7.38)	6.30 (6.14–6.64)
39	Nleu							7.27 (6.73–7.92)	6.97 (6.37–7.63)
40	BALA							8.67 (8.15–9.31)	7.56 (6.88–8.27)
41	Pro							12.31 (11.60–13.26)	10.83 (9.79–11.84)
42	CAPS							12.60 (11.75–13.58)	10.95 (10.00–12.84)

The RSH values were calculated from the conductivity detection data, as obtained in the analytical column from the ITP runs performed in the electrolyte systems described in Table 1. The zones of chloride (the leading anion) and carbonate served as references (see also Fig. 2). The ranges reflect fluctuations in the data obtained from the runs with samples of different compositions, in which a given constituent was present, and drifts of the detection signal (drifts of the zone plateaus) during a particular run.

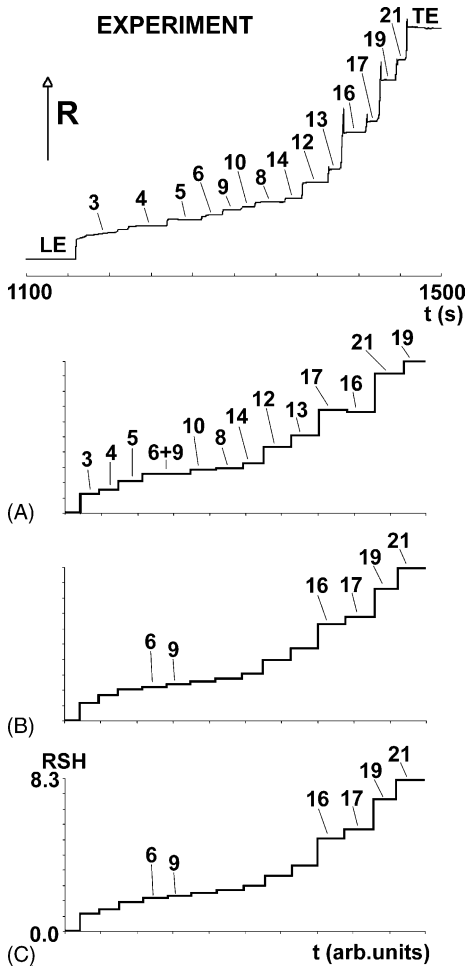

Fig. 4. Predictions of the migration order of a group of discrete spacers at pH = 7.0 using various sets of the input data. For the input data employed, see Table 5. A reference isotachopherogram to the ITP separation of the spacers (the electrolyte system no. 2, Table 1) was obtained from the response of the conductivity detector of the analytical column. The sample, containing each of the constituents (with the exception of carbonate) at a 50 μmol/l concentration, was loaded by a 30 μl internal sample loop of the injection valve. The driving currents were stabilized at 200 and 40 μA in the preseparation and analytical columns, respectively.

illustrates an isotachopherogram as obtained from the separation of a group of the spacing constituents at pH = 7.0 and its predictions (Fig. 4). Here, to eliminate impacts of extremes on the prediction, we took the medians of their pK_a and ionic mobility values as found in the literature (A, in Table 5). A comparison of the corresponding prediction (A, in Fig. 4) with the isotachopherogram shows that such a choice of the input data did not lead to a satisfactory agreement. Nevertheless, a set of the literature data could be chosen (B, in Table 5) that provided very good results in this respect (B, in Fig. 4). In spite of the fact that this data set gave the prediction that agreed very well with the ITP run performed at pH = 7.0, it failed in providing correct predictions of the migration orders of some of these constituents in other electrolyte systems.

As already mentioned above, the detection data as obtained from the ITP separations of mixtures of the studied constituents were employed in the calculations of their ionic mobilities and pK_a values. The calculation procedure, described in the above sections, provided the ionic mobilities and pK_a values (Table 3) that, in general, gave best fits of the predictions with the ITP separations within the studied pH range. This, for example, documents one of the predictions carried out for pH = 7.0 (C, in Fig. 4). In this context, it seems appropriate to note that the ionic mobilities and pK_a values obtained from the experimental data gave, contrary to a selected set of the literature data (B, in Fig. 4), the predictions that matched the actual migration orders in the ITP separations carried out in other electrolyte systems as well. This is understandable because the predictions used the input data acquired under the working conditions that agreed with those under which the ITP separations were performed.

For boric acid and ADA, the ionic mobility and pK_a data of adequate qualities could not be obtained from the ITP experiments. For the former constituent, forming complexes with hydroxyl groups containing compounds in the electrophoretic separations (see, e.g. [64]), this was due to the fact that contributions of Tris–borate and BTP–borate complex species to the effective mobilities of borate at pH = 8.0–9.5 (the separations in the electrolyte systems nos. 4–7, Table 1) could not be ignored. As the complex equilibria involved were not reflected in the relationships used in the calculations of the ionic mobilities and pK_a values (Eqs. (10) and (11)), the experimental data a priori could not provide correct values. On the other hand, ADA, having within the studied pH interval the effective mobilities very close to those of carbonate, was not usually well resolved from this anion and,

Table 5
Predictions of the migration orders of the spacing constituents in the ITP stack at pH = 7.0

Spacer	Experiment		Prediction A				Prediction B				Prediction C			
	Stack	RSH	Stack	RSHA	pK (i)	m (i)	Stack	RSHB	pK (i)	m (i)	Stack	RSHC	pK (i)	m (i)
Carb	I	1.00	I	1.00	6.35 (1)	46.1 (1)	I	1.00	6.35 (1)	46.1 (1)	I	1.00	6.35 (1)	46.1 (1)
					10.33 (2)	71.8 (2)			10.33 (2)	71.8 (2)			10.33 (2)	71.8 (2)
PIPES	II	1.30	II	1.22	6.37 (2)	41.6 (2)	II	1.22	6.37 (2)	41.6 (2)	II	1.22	6.37 (2)	41.6 (2)
			pH inversion ↕								pH inversion ↕			
Asp	III	1.55	III	1.64	3.90 (1)	30.9 (1)	III	1.71	3.90 (1)	30.1 (1)	III	1.64	3.90 (1)	30.9 (1)
					9.97 (2)	54.7 (2)			10.00 (2)	55.4 (2)			10.00 (2)	55.4 (2)
Glu	IV	1.74	IV–V	1.99	4.30 (1)	27.4 (1)	IV	1.83	4.38 (1)	28.9 (1)	IV	1.87	4.32 (1)	28.5
					9.80 (2)	53.2 (2)			9.96 (2)	49.6 (2)			9.96 (2)	53.0
			Mixed zone ↕											
Cacd	V	1.95	IV–V	1.99	6.21	29.9	V	1.96	6.18	29.9	V	2.00	6.33	30.3
MES	VI	2.06	VI	2.20	6.14	27.4	VI	2.12	6.10	28.0	VI	2.12	6.18	28.3
			pH inversion ↕				pH inversion ↕				pH inversion ↕			
Apm	VII	2.24	VII	2.28	4.30 (1)	25.0 (1)	VII	2.28	4.30	25.0	VII	2.28	4.30	25.0
					9.80 (2)	44.0 (2)			9.80	44.0			9.80	44.0
POPSO	VIII	2.38	VIII	2.52	7.26	36.9	VIII	2.52	7.26	36.9	VIII	2.52	7.26	36.9
			pH inversion ↕				pH inversion ↕				pH inversion ↕			
MOPSO	IX	3.01	IX	3.35	6.85	23.8	IX	3.25	6.79	23.8	IX	3.08	6.95	26.6
MOPS	X	3.53	X	3.90	7.18	24.4	X	3.85	7.16	24.4	X	3.61	7.23	26.9
DIPSO	XI	4.97	XII	5.09	7.59	25.0	XI	5.09	7.59	25.0	XI	5.09	7.59	25.0
			m inversion ↕											
HEPES	XII	5.40	XI	5.20	7.43	21.8	XII	5.51	7.51	21.8	XII	5.59	7.61	23.2
Gly-Gly	XIII	7.02	XIV	7.58	8.28	31.5	XIII	7.00	8.20	31.5	XIII	7.20	8.24	31.9
							pH inversion ↕				pH inversion ↕			
HEPPSO	XIV	7.80	XIII	6.99	7.82	22.0	XIV	8.10	7.99	22.0	XIV	8.25	8.01	22.0

For the assignments of the codes of constituents see Table 2. Stack: the roman numeral identifies the migration position of a particular constituent in the ITP stack; A: the prediction using the medians of pK_a and m values taken from refs. [42,49,50,52,57]; B: the prediction using the literature pK_a and m values leading to the same migration order as the ITP experiments at pH = 7.0 (the electrolyte system no. 2, in Table 1); C: the prediction using the pK_a and m values calculated from the experimental data obtained in this work (for details, see the text). pH inversion ↕, m inversion ↕ and mixed zone ↕ are migration "anomalies" [2,53,56], as found for particular pairs of the constituents in the calculation of the migration order (see also the text).

consequently, only less reliable data were available for this constituent. Therefore, the use of boric acid and ADA in mixtures of discrete spacers was based only on the experimental data as obtained at a particular pH value.

4.2. Uncertainty in pH of the leading electrolyte and the prediction of the migration order of the constituents in the ITP stack

An actual pH value of the leading electrolyte solution is known with a small uncertainty that is associated with the pH measurement [65,66]. Therefore, the steady-state parameters of the zones of the spacing constituents and predictions of their migration orders in the ITP stacks calculated for a given pH value of the leading electrolyte may be, in fact, compared with the experimental data obtained at a slightly different pH value. An impact of such a pH uncertainty on the predictability of the migration order is apparent from isotachopherograms shown in Fig. 5. Here, we can see that the ITP separation performed at pH = 6.50 (the pH value of the leading electrolyte was measured immediately before the separation) agreed with the prediction calculated for pH = 6.54. At the same time, the predictions indicate a significant sensitivity of the migration order of this group of constituents to small pH fluctuations at pH values close to 6.50.

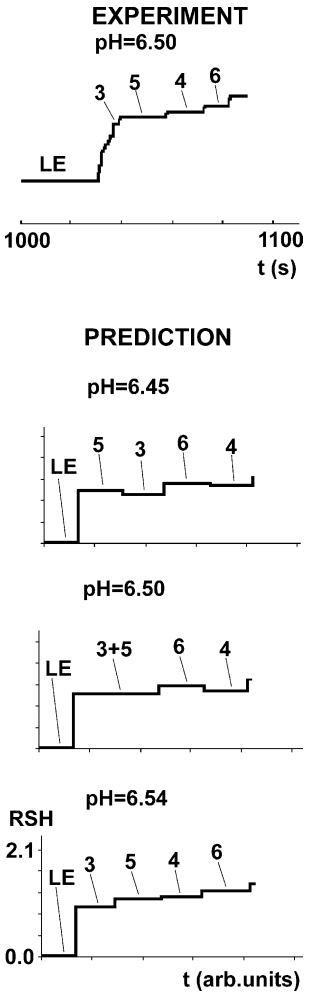

Fig. 5. Impacts of small differences in the pH value of the leading electrolyte on the predictions of the migration order of carbonate (3), PIPES (4), aspartate (5) and glutamate (6) in the ITP stack. The predictions were calculated using the ionic mobilities and pK_a values obtained from the ITP experiments performed in this work (Table 3). A reference isotachopherogram to the ITP separation of these constituents (the electrolyte system no. 1, Table 1) was obtained from the response of the conductivity detector of the analytical column. The sample, containing each of the constituents (with the exception of carbonate) at a 50 μmol/l concentration, was loaded by a 30 μl internal sample loop of the injection valve. The driving currents were stabilized at 200 and 40 μA in the preseparation and analytical columns, respectively.

Apparently, in instances like this it was hardly possible to make conclusions regarding the agreement of the prediction with the corresponding ITP experiment. On the other hand, these results indicate that the prediction of the migration order performed for a particular pH value should be complemented by the ones performed for pH values from a close neighborhood. An evaluation of an inherent uncertainty in the pH value of the leading electrolyte solution on the separation of a given group of the spacing constituents carried out in this way, in fact, characterizes a robustness of their migration configuration with respect to small pH fluctuations. In addition, this step can identify the constituents that could behave critically in the ITP separations performed within a given pH interval [53,59] and, consequently, facilitate the choice of a mixture of discrete spacers suitable for a particular pH.

4.3. Choice of a multi-component mixture of the spacing constituents

A practical applicability of the elaborated procedure to the choice of multi-component mixtures of discrete spacers was examined for the all electrolyte systems employed in this work. The results obtained at pH = 10.0 (the electrolyte system no. 8, in Table 1) were chosen as illustrative because under these acid–base conditions the complete group of the constituents taken into our study (Table 2) could be evaluated. Relevant isotachopherograms from the conductivity and UV-photometric absorbance detectors as obtained from the separation of a 20 component mixture of discrete spacers (a maximum number of the studied constituents that could be resolved in one ITP run at pH = 10.0) are given in Fig. 6. The records obtained from the UV-detector (Fig. 5B and C) illustrate known roles of the discrete spacers in minimizing interferences in the photometric detection of analytes caused by UV light-absorbing impurities present in the electrolyte solutions (see, e.g. [3,6,13]). On the other hand, the one obtained from the response of the conductivity detector (Fig. 6A) shows how this particular mixture of the spacing constituents covered the span of the effective mobilities determined by the leading and terminating anions. ITP experiments and the calculations provided also the data for the remainder of the studied constituents and their positions in the ITP stack are marked on the isotachopherogram in Fig. 6A. They can be considered as alternatives in situations when one or several of the constituents present in the mixture fail in providing required spacing effects.

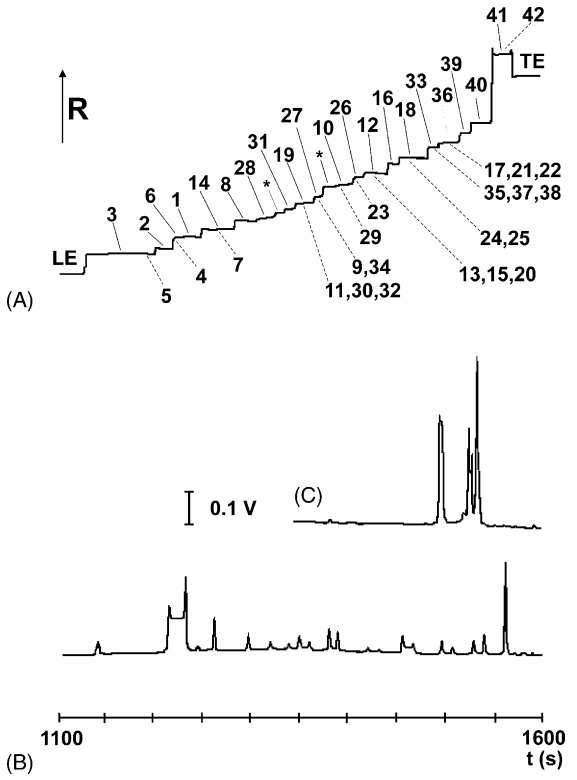

Fig. 6. Isotachopherograms obtained from the separation of a 20 constituent mixture of discrete spacers at pH = 10.0: (A) the record obtained from the response of the conductivity detector of the analytical column; (B) the record obtained from the same run as in (A) from the response of the UV detector coupled to the analytical column; (C) the record as registered from the UV detector from the run when the discrete spacers were not loaded. The concentrations of the discrete spacers in the injected sample (a 30 μl volume by the sample loop of the injection valve) were 50 μmol/l. The separations were carried out in the electrolyte system no. 8 (Table 1) with the driving currents stabilized at 200 and 40 μA in the preseparation and analytical columns, respectively. Dashed lines indicate the migration positions of the alternative spacing constituents. For the zone assignments, see Table 2. The prediction of the migration order of the discrete spacers along with the calculated steady-state parameters of their zones are given in Table 6.

Table 6
The migration order of the constituents present in a mixture of discrete spacers for pH = 10.0 and its prediction

Spacer	Experiment		Prediction			
	Stack	RSH	Stack	RSH	pH	$\bar{m}$
Chloride (LA)		0		0	10.00	79.1
Carb (3)	I	1.00	I	1.00	10.10	55.6
ADA (2)	II	1.24	II	–	–	–
Glu (6)	III	1.78	IV	1.94	10.15	43.4
AMSA (1)	IV	1.81	III	1.89	10.12	44.0
POPSO (14)	V	2.28	VI	2.71	10.17	36.9
			pH inversion ↕			
Apm (8)	VI	2.59	V	2.51	10.18	38.4
Tau (28)	VII	2.73	VII	3.23	10.21	33.4
Boric (31)	VIII	3.18	VIII	–	–	–
Gly-Gly (19)	IX	3.47	IX	3.56	10.22	31.6
Asn (27)	X	3.78	X	4.06	10.25	29.1
MES (10)	XI	4.32	XI	4.24	10.26	28.3
Metso (26)	XII	4.72	XIII	4.72	10.29	26.4
MOPSO (12)	XIII	4.92	XII	4.67	10.28	26.6
DIPSO (16)	XIV	5.37	XIV	5.13	10.30	25.0
TAPSO (18)	XV	5.66	XV	5.44	10.32	23.9
AMPSO (33)	XVI	6.17	XVI	6.41	10.38	21.3
			Enforced system ↕			
Cit (36)	XVII	6.41	XVII	6.40	10.40	21.4
Nleu (39)	XVIII	6.87	XVIII	6.94	10.44	20.1
BALA(40)	XIX	7.37	XIX	7.31	10.53	19.3
Pro (41)	XX	10.71	XX	9.42	10.79	15.9
OH^- (TA)		–		–	–	–

For the assignments of the spacers, see Table 2. Stack: the roman numeral identifies the migration position of the constituent in the ITP stack; the prediction used the pK_a and m values obtained in this work (Table 3); pH inversion ↕ and enforced system ↕ are migration "anomalies" [2,53,56], as found for particular pairs of the constituents in the prediction of the migration order (see also, the text).

For reasons apparent from the above discussion, we preferred in the calculations aimed at selecting multi-component mixtures of discrete spacers the data obtained in this work. Using these data, the steady-state parameters of the zones of the studied constituents were calculated and their migration orders predicted. This introductory step identified the constituents that led to the ITP migration configurations of low robustness with respect to small pH fluctuations (a majority of the alternative spacers in Fig. 6A) and, consequently, reduced the number of candidates from which a multi-component mixture of the spacing constituents could be chosen. In this way a mixture consisting of 18 constituents suitable for pH = 10.0 was found. Using the data obtained from the ITP experiments, it was complemented by borate and ADA (see above).

The prediction obtained for pH = 10.0 (Table 6) agreed well with the corresponding ITP run (Fig. 6). However, the predicted migration orders of Glu and AMSA, POPSO and Apm, and Metso and MOPSO differed from those obtained experimentally. These

differences can be very likely ascribed to small uncertainties in their ionic mobilities because the pK_a values (with the exception of Glu and Apm) do not contribute to the effective mobilities at pH = 10.0. Performing the predictions for the full spans of the ionic mobility data of these constituents (see Table 3), we found combinations giving agreements of the predicted and experimental migration orders. From a practical point of view, however, this was less effective as only potential discrepancies in the migration orders could be identified in this way. This is due to the fact that the choice of the input data providing for a particular electrolyte system the prediction that perfectly agreed with the experiment required a feedback from the ITP experiments performed in this system. An analogous step was required for the same constituents in other electrolyte systems since other values of the ionic mobilities and/or pK_a values gave agreements of the predictions with the experiments. This, in fact, set limits of the calculation based choice of multi-component mixtures of discrete spacers as developed in this work.

5. Conclusions

The calculations of the steady-state parameters of the ITP zones of the separated constituents and predictions of their migration orders in the ITP stack offer a convenient tool in the choice of mixtures of discrete spacers. Its use is effective when the calculations are combined with the ITP experiments that provide references with which the calculated data and predictions can be compared. This approach, however, favors that a limited number of constituents is found that forms a pool from which a mixture of discrete spacers suitable for a particular analytical problem is chosen. A group of 42 anionic and zwitterionic constituents chosen for our study (Table 2) provided mixtures of the spacing constituents that covered well the effective mobility spans defined by the leading and terminating anions employed in the ITP separations performed at pH = 6.5–10.0. In this context, we should note that this group is opened and when needed other constituents of required electromigration and detection properties can extend it.

The ionic mobility and pK_a data available for some of the studied constituents in the literature scatter significantly and their use in the calculations resulted in controversial predictions of the migration orders of the constituents in the ITP stacks. The ITP experiments performed in this work, primarily aimed at assessing the separabilities of the studied spacing constituents, provided the electromigration data that performed much better in this respect. This is understandable because in this instance they were acquired under the experimental conditions that agreed with those under which the separations were carried out. In a general sense, however, they have inherently restricted applicabilities unless appropriately corrected, for example, for the ionic strength effects.

An actual pH value of the leading electrolyte solution is known with a small uncertainty. This uncertainty becomes important for the constituents that change their migration orders in a close neighborhood of a particular pH value. Performing the predictions of the migration orders for a certain pH interval in which this pH value is included can identify this problem. This step in the choice of discrete spacers is very practical as it, in fact, determines the candidates from which the mixture can be chosen.

The ionic mobility and pK_a data preferred in our calculations were obtained with some uncertainties attributable to the experimental conditions (e.g. the use of the contact conductivity detection to the acquisition of the primary data; reproducibilities with which the leading electrolyte solutions are prepared; slightly variable contents of carbonate in the electrolyte solutions) and the calculation procedure employed. These uncertainties may prevent the predictions of correct migration orders of some constituents of close ionic mobilities (see the above discussion regarding the choice of multi-component mixtures of discrete spacers). It seems reasonable to assume that their roles can be diminished by using a refined ITP measurement procedure as elaborated, for example, by Gaš et al. [48]. For the studied constituents and the separating conditions employed in this work, however, this should be accompanied by highly precise measurements of pH of the electrolyte solutions while minimizing contents of carbonate in these solutions, for example, using means as proposed by Verheggen et al. [58]. Obviously, an enhanced quality of the electromigration data attainable in this way is paid for by a loss of the simplicity of the measurement procedure.

Acknowledgements

This work was supported by Merck (Darmstadt, Germany), J&M (Aalen, Germany) under the project No. 720.830-1-21/9 and, in part, by grants from the Slovak Grant Agency for Science under the projects Nos. 1/0087/03 and 1/0061/03.

References

[1] F.M. Everaerts, J.L. Beckers, Th.P.E.M. Verheggen, Isotachophoresis. Theory, Instrumentation and Applications, Elsevier, Amsterdam, 1976.
[2] P. Boček, M. Deml, P. Gebauer, V. Dolník, Analytical Isotachophoresis, VCH, Weinheim, 1988.
[3] M. Svoboda, J. Vacík, J. Chromatogr. 119 (1976) 539.
[4] S.G. Hjalmarsson, A. Baldesten, CRC Crit. Rev. Anal. Chem. 11 (1981) 261.
[5] L. Arlinger, R.J. Routs, Sci. Tools 17 (1970) 21.
[6] L. Arlinger, J. Chromatogr. 91 (1974) 785.
[7] P. Delmotte, J. Chromatogr. 165 (1979) 87.
[8] G. Eriksson, Anal. Biochem. 109 (1980) 239.
[9] P. Delmotte, Sep. Purif. Method 10 (1981) 29.
[10] F. Oerlemans, C. Debruyn, F. Mikkers, T. Verheggen, F. Everaerts, J. Chromatogr. 225 (1981) 369.
[11] D. Kaniansky, V. Madajová, M. Hutta, I. Žilková, J. Chromatogr. 286 (1984) 395.
[12] G. Schmitz, U. Borgmann, G. Assmann, J. Chromatogr. 320 (1985) 253.
[13] D. Kaniansky, V. Madajová, J. Marák, E. Šimuničová, I. Zelenský, V. Zelenská, J. Chromatogr. 390 (1987) 51.
[14] I. Zelenský, V. Zelenská, D. Kaniansky, J. Chromatogr. 390 (1987) 111.
[15] I. Zelenský, D. Kaniansky, P. Havaši, Th.P.E.M. Verheggen, F.M. Everaerts, J. Chromatogr. 470 (1989) 155.
[16] M. Hutta, J. Marák, D. Kaniansky, J. Chromatogr. 509 (1990) 271.
[17] P. Kopáček, D. Kaniansky, J. Hejzlar, J. Chromatogr. 545 (1991) 461.
[18] M. Hutta, D. Kaniansky, E. Šimuničová, V. Zelenská, V. Madajová, A. Šišková, J. Radioanal. Nucl. Chem. Art. 163 (1992) 87.
[19] D. Kaniansky, I. Zelenský, J. Chromatogr. 638 (1993) 225.
[20] S.J. Chen, M.L. Lee, J. Microcolumn Sep. 10 (1998) 423.
[21] I. Nagyova, D. Kaniansky, J. Chromatogr. A 916 (2001) 191.
[22] D. Kaniansky, J. Marák, P. Rajec, A. Švec, M. Koval', M. Lúčka, G. Sabanoš, J. Chromatogr. 470 (1989) 139.
[23] D. Kaniansky, P. Rajec, A. Švec, J. Marák, M. Koval', M. Lúčka, Š. Franko, G. Sabanoš, J. Radioanal. Nucl. Chem. Art. 129 (1989) 305.
[24] D. Kaniansky, P. Havaši, J. Marák, R. Sokolík, J. Chromatogr. 366 (1986) 153.
[25] D. Kaniansky, P. Havaši, F. Iványi, J. Marák, J. Chromatogr. A 709 (1995) 69.
[26] L. Arlinger, J. Chromatogr. 119 (1976) 9.
[27] J. Caslavska, W. Thormann, Electrophoresis 15 (1994) 1176.
[28] T. Hirokawa, Y. Kiso, J. Chromatogr. A 658 (1994) 343.
[29] M. Hutta, D. Kaniansky, E. Kovalčíková, J. Marák, M. Chalányová, V. Madajová, E. Šimuničová, J. Chromatogr. A 689 (1995) 123.
[30] D. Kaniansky, J. Marák, J. Chromatogr. 498 (1990) 191.
[31] D. Kaniansky, J. Marák, V. Madajová, E. Šimunićová, J. Chromatogr. 638 (1993) 137.
[32] M. Danková, D. Kaniansky, S. Fanali, F. Iványi, J. Chromatogr. A 838 (1999) 31.
[33] M. Danková, S. Strašík, M. Molnárová, D. Kaniansky, J. Marák, J. Chromatogr. A 916 (2001) 143.
[34] J. Marák, J. Laštinec, D. Kaniansky, V. Madajová, J. Chromatogr. 509 (1990) 287.
[35] F. Acevedo, J. Chromatogr. 470 (1989) 407.
[36] F. Acevedo, Z. Goitom, J. Chromatogr. 545 (1991) 343.
[37] F. Acevedo, J. Chromatogr. 545 (1991) 391.
[38] J. Caslavska, P. Gebauer, W. Thormann, Electrophoresis 15 (1994) 1167.
[39] G. Schmitz, C. Mollers, Electrophoresis 15 (1994) 31.
[40] T. Hirokawa, Y. Kiso, J. Chromatogr. 252 (1982) 33.
[41] T. Hirokawa, M. Nishino, Y. Kiso, J. Chromatogr. 252 (1982) 49.
[42] T. Hirokawa, M. Nishino, N. Aoki, Y. Kiso, Y. Sawamoto, T. Yagi, J. Akiyama, J. Chromatogr. 271 (1983) D1.
[43] V. Kašička, J. Vacík, Z. Prusík, J. Chromatogr. 320 (1985) 33.
[44] R.A. Mosher, D.A. Saville, W. Thormann, The Dynamics of Electrophoresis, VCH, Weinheim, 1992.
[45] J.H.P.A. Martens, J.C. Reijenga, J.H.M.T. Boonkkamp, R.M.M. Mattheij, F.M. Everaerts, J. Chromatogr. A 772 (1997) 49.
[46] J.L. Beckers, J. Chromatogr. 320 (1985) 147.
[47] P. Bednář, Z. Stránský, J. Ševčík, V. Dostál, J. Chromatogr. A 831 (1999) 277.
[48] B. Gaš, J. Zuska, J. Vacík, J. Chromatogr. 470 (1989) 69.
[49] T. Hirokawa, T. Gojo, Y. Kiso, J. Chromatogr. 369 (1986) 59.
[50] T. Hirokawa, Y. Kiso, B. Gaš, I. Zusková, J. Vacík, J. Chromatogr. 628 (1993) 283.
[51] J. Pospíchal, M. Deml, P. Boček, J. Chromatogr. 390 (1987) 17.
[52] J. Pospíchal, P. Gebauer, P. Boček, Chem. Rev. 89 (1989) 419.
[53] P. Gebauer, P. Boček, J. Chromatogr. 267 (1983) 49.
[54] D. Kaniansky, V. Madajová, I. Zelenský, S. Stankoviansky, J. Chromatogr. 194 (1980) 11.
[55] T. Hirokawa, S. Kobayashi, Y. Kiso, J. Chromatogr. 410 (1987) 279.
[56] V. Jakúbek, MScThesis, Comenius University, Bratislava, 1992.
[57] T. Hirokawa, T. Gojo, Y. Kiso, J. Chromatogr. 390 (1987) 201.
[58] T.P.E.M. Verheggen, J.C. Reijenga, F.M. Everaerts, J. Chromatogr. 260 (1983) 471.
[59] F.E.P. Mikkers, F.M. Everaerts, J.A.F. Peek, J. Chromatogr. 168 (1979) 293.
[60] F.M. Everaerts, P.J. Rommers, J. Chromatogr. 91 (1974) 809.

[61] D. Kaniansky, PhD Thesis, Comenius University, Bratislava, 1981.
[62] E. Kenndler, Anal. Chim. Acta 173 (1985) 239.
[63] D. Kaniansky, J. Marák, J. Laštinec, J.C. Reijenga, F.I. Onuska, J. Microcolumn Sep. 11 (1999) 141.
[64] P. Schmitt-Kopplin, N. Hertkorn, A.W. Garrison, D. Freitag, A. Kettrup, Anal. Chem. 70 (1998) 3798.
[65] R.G. Bates, Determination of pH. Theory and Practice, Wiley, New York, 1964.
[66] R. Naumann, C. Alexander-Weber, R. Eberhardt, J. Giera, P. Spitzer, Anal. Bioanal. Chem. 374 (2002) 778.
[67] D. Kaniansky, I. Nagyová, J. Marák, Acta Univ. Matthaei Belii. Chém. 3 (1999) 59.